EUROPEAN ORGANIZATION FOR NUCLEAR RESEARCH
ORGANISATION EUROPEENNE POUR LA RECHERCHE NUCLEAIRE

CERN - PS DIVISION

PS/RF/ Note 2001-012

MEASUREMENT OF THE LONGITUDINAL COUPLING IMPEDANCE FOR THE PS ELECTROSTATIC SEPTUM 23

F. Caspers, A. Mostacci

Abstract

In the frame of general PS machine impedance evaluation, the septum PESEH23 has been measured using the classical coaxial wire method with and without matching resistors.
In order to reduce undesirable resonance effects from "cavities" formed by a gap between the main septum chamber of quasi-elliptical cross-section and the end plates of the vacuum tank, already RF contact fingers were mounted on a metal plate in about 10-15 cm radial distance from the beam. Measured data are compared with HFSS simulations and possible further improvements to push the lowest resonance mode well above 1 GHz are discussed.

Geneva, Switzerland
October 2001

1 Introduction and motivation

A constant and persistent effort is required to improve whenever possible the beam coupling impedance of all PS machine elements. This is due to the fact that the PS machine has undergone many upgrades during its evolution over the past decades. As a consequence the beam intensity has been augmented by several orders of magnitude and bunch lengths became shorter. Obviously more stringent requirements for the impedance budget result from these improvements. Since there are nearly always certain elements of the PS machine taken out for repair or upgrade, one has to use the opportunity the measure the impedance on the bench and if required, implement or foresee further ameliorations.

In the framework of the consolidation project of the electrostatic septa in the PS ring [1], the septum PESEH23 became available for impedance bench measurements during the summer 2000. Usually the measurement job is not at all straightforward; it requires individual adaptation for the particular Device Under Test (DUT) and the use of different approaches even on the same test object. On top of that, often there is little time available for measurements since the object is more or less radioactive.

Usual techniques and advises to correctly perform impedance bench measurements are summarised in [2]. In the present paper we report about the results of measurements of the longitudinal coupling impedance by means of the so called "coaxial wire method". A description of the actual set-up and the measurement procedure are given in sec. 2. The raw data require careful evaluation (sec. 2.1-2.2) and a comparison with numerical simulation results by HFSS [4] is very helpful for a good understanding (sec. 2.3). Eventually a proposal for possible improvements is discussed in sec. 3.

A schematic drawing of the device is shown in Fig. 1 which gives a transverse view (left picture) and a longitudinal view (right picture). The beam travels in an elliptical vacuum chamber before entering into the septum where the elliptical chamber is cut by an molybdenum foil (i.e. the "septum" according to Fig. 1) in front of the High Voltage (H.V.) electrode. The photo of the beam pipe inside the device is shown in Fig. 2 (left picture) where the H.V. electrode and the septum foil are clearly visible. The openings on the right hand side of the pipe are venting holes and their impact will be seen in the measurements. In the following we refer to the septum as the whole device and not strictly the molybdenum foil, as indicated in Fig. 1. The septum is contained in a tank with circular flanges which have to be electrically connected with the septum itself. For this purpose, some RF-fingers were mounted on the septum extremity, as shown Fig. 2 (right picture). Those contacts form a kind of cavity with the external tank flanges: the effect of this cavity will be discussed in details.

2 Measurements

A copper wire (rod) is placed on the axis of the DUT and a Vector Network Analyser (VNA) measures the transmission coefficient S_{21} between the two extremities. Two sets of measurements are performed: one with a copper wire having a diameter of 0.4 mm and one with a much thicker wire (actually a rod) with 1 cm diameter. The wire (rod) is aligned to the centre of the tank flanges (see Fig. 1); in general this is not the centre of the elliptical vacuum chamber, since during machine operation the chamber inside the septum is moved due to machine optics requirements. The measurements have been carried out on PESEH23 in operating conditions, i.e. with 1 cm horizontal offset between the flange centre and the ellipse centre. A great caution had to be exercised, when placing the wire inside the vacuum chamber without damaging the very thin septum foil.

The coaxial transmission line formed by DUT + wire is mismatched with respect to

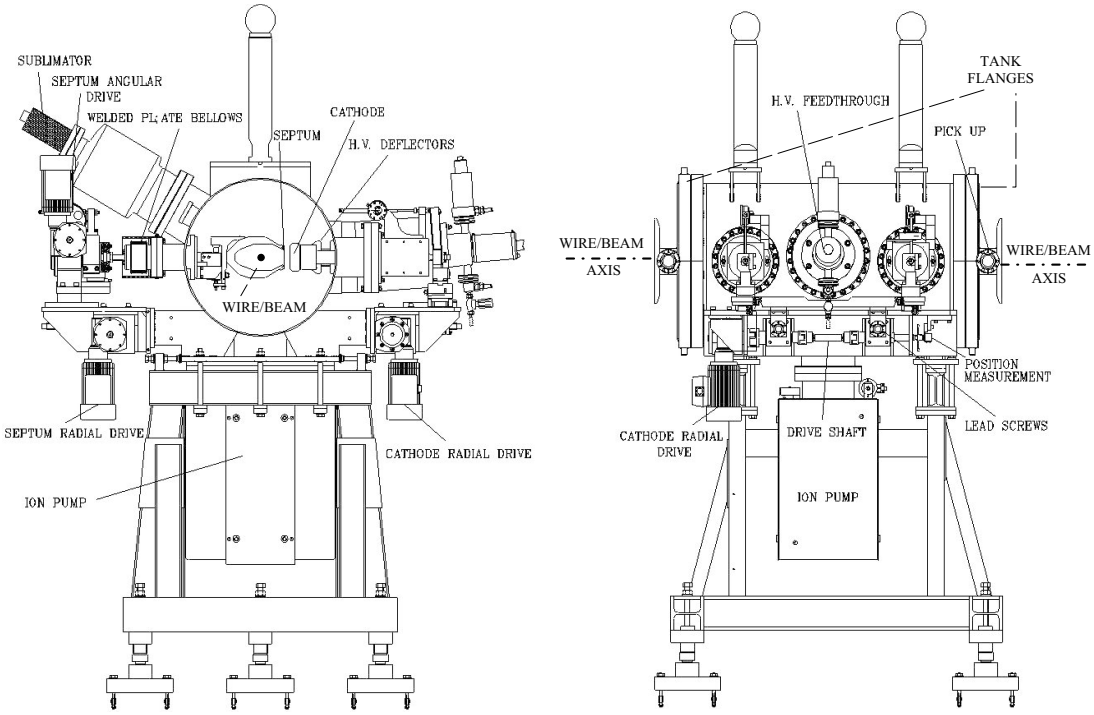

Figure 1: Simplified drawing of the whole septum. The left picture gives a transverse view of the device: the quasi-elliptical vacuum chamber inside the septum tank is clearly visible. The right picture is a view "parallel" to the beam axis. The wire for the bench measurement is aligned at the centre of the circular tank flanges (which does not necessarily correspond to the centre of the elliptical chamber).

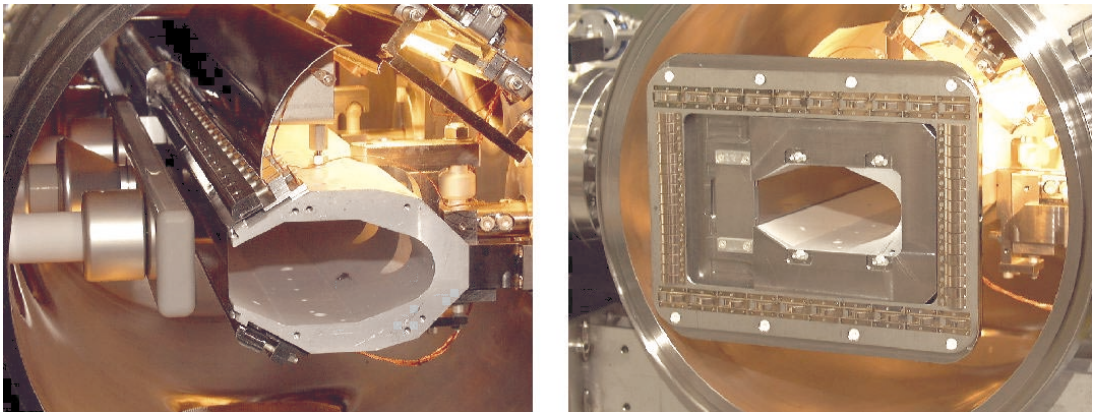

Figure 2: Detailed septum views. The left picture shows the inside part of the septum tank: the nearly elliptical beam pipe is "cut" by an molybdenum foil. The pumping holes are visible in the right part of the pipe. The right picture shows the end of the tank, where the external (tank) flanges are put in place. The RF-contacts assure a good electrical transition between septum and the external flange.

the instrument (VNA, 50 Ω generator and load impedance) and some matching resistors have been used in this case (see sec. 2.1). The losses in the resistors affect the measurements and thus to get rid of their influences, the rod measurements were instead performed without matching resistors.

To evaluate the coupling impedance, the raw data are analysed with the so called "logarithmic formula":

$$Z_{log} = -2Z_c \ln\left(\frac{S_{21}^{DUT}}{S_{21}^{REF}}\right) \tag{1}$$

where Z_c is the characteristic impedance of the coaxial line and S_{21} is the transmission coefficient (measured by the VNA). REF stands for REFerence measurement; such a reference measurement in a smooth, homogeneous beam pipe has not been done for practical reasons. We assumed, instead, for the reference a lossless line of length L (that is $S_{21}^{REF} = e^{-j\omega L/c}$) where L is the mechanical distance between the connectors joining the wire (rod) extremities with the cables from the network analysers. This delay has been included in the raw data via the time delay correction function of the network analyser; thus, all the S_{21} data discussed/used in the following are meant to be $S_{21}^{DUT}/S_{21}^{REF}$.

2.1 Wire measurements

In order to get the correct value of the matching resistor, we need a measurement of the impedance Z_c of the wire in the DUT. Then, the resistance Z_{match} satisfies simply the matching condition [3]:

$$Z_c = Z_{match} + 50\ \Omega.$$

To measure Z_c we performed a kind of "Time Domain Reflectometry", using the time domain option of the HP8753D network analyser. We measured the signal reflected by the unmatched transmission line with a synthesised (unitary) step excitation, the so called "low frequency step" in the VNA jargon. The calibrated S_{11} for the (unmatched) coaxial line is shown in Fig. 3 as a function of the delay along the transmission line; where the different "stairs" are the multiple reflections at the opposite end of the structure. One can see clearly the contribution of the "entrance cavity" and "exit cavity" as well as the influence of the periodically spaced lateral venting holes (about 4 cm diameter) in the ellipse like cross section beam pipe inside the septum tank. From the amplitude $\Delta\Gamma$ of the reflection coefficient it is possible to get the impedance of the line Z_c, i.e.

$$Z_c = Z_0\frac{1+\Delta\Gamma}{1-\Delta\Gamma} = Z_0\frac{1+0.714}{1-0.714} = 299\ \Omega, \tag{2}$$

since $Z_0 = 50\ \Omega$. According to Eq. (2.1), $Z_{match} = Z_c - Z_0 = 249\ \Omega$; for practical reasons, then, the two matching resistors actually soldered between the wire and the connectors are of 270 Ω.

After soldering the matching resistors on each side of the copper wire, the transmission coefficient S_{21} looks like in Fig. 4. The upper plot shows its magnitude (in db) when the low frequency ohmic losses on the matching resistor are corrected away. The lower plot shows the phase of S_{21} after the time delay correction according to the (mechanical) length of the line (which is roughly 1.15 m). The notches pointed by the two arrows are due to electromagnetic energy trapped in the two passive cavities between the septum ends and the tank flanges (see Fig. 2). The two cavities are coupled by the coaxial structure and the first notch shows the typical "double peaks" pattern of coupled cavities oscillations. The higher frequency notch (second arrow) is quite wide and this may be due to coupled oscillation or to a sampling inaccuracy. At the time the write-up was done (several months after the measurements) more data were not available since the septum

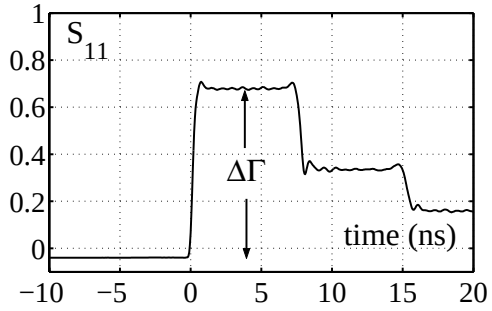

Figure 3: Reflection coefficient measurements in the time domain. The plot shows multiple reflections in the non-matched coaxial line obtained by inserting a wire (0.4 mm diameter) along the DUT axis. Each plateau has the same typical structure of an undulation with small overshoots at the beginning and at the end. The overshoots are due to the entrance and exit passive cavities formed by the contacts and the external tank flanges, while the undulation is due to the venting holes. The values of the matching resistors are computed from $\Delta\Gamma$ ($\Delta\Gamma = 0.174$).

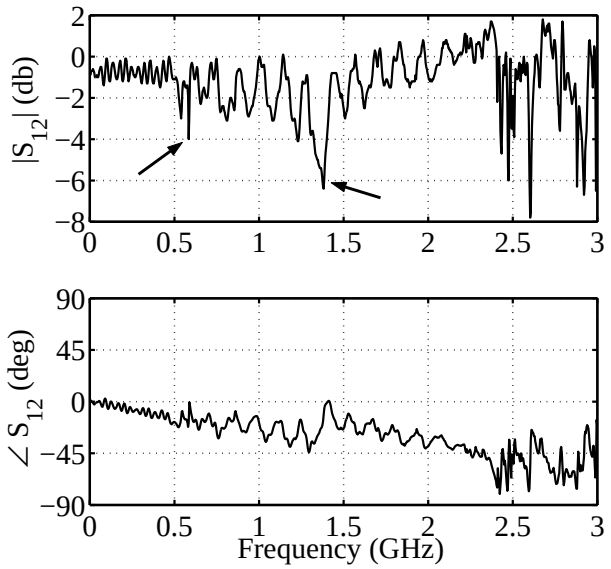

Figure 4: Transmission coefficient (S_{21}) versus frequency. A copper wire (0.4 mm diameter) is placed along the DUT axis. Matching resistors have been mounted at each end of the wire. The amplitude (upper plot) has been corrected from the low frequency losses on the resistors. The lower plot shows the phase of the S_{21}, corrected according the distance between the two VNA connectors, that is 1.1471 m (time delay correction). The arrows indicate two (unexpected) resonances.

is not anymore accessible for bench measurements. The other notches at high frequency (around 2.5 GHz and above) are the signature of higher order propagating modes. The ripple at low frequencies (below 500 MHz) is due to the imperfect matching as mentioned above since the resistors actually soldered have not exactly the theoretical value. To get the plot of Fig. 4, the raw data for $|S_{21}|$ are artificially modified: the plot is shifted up in order to subtract the ohmic losses on the matching resistors at low frequency. Unfortunately, their losses changes with frequencies and this explains the (unphysical) behaviour

of an $|S_{21}|$ greater than 0 db above 1.5 GHz.

The longitudinal coupling impedance can be calculated using the raw data of the transmission coefficient in Eq. (1) with Eq. (2); its real part Z_{real} is shown in Fig 5. The peaks (pointed by the arrows) correspond obviously to the notches of the $|S_{21}|$ and they are due to the transition between the tank flanges and the septum extremities. These two passive cavities gives the main contributions to the coupling impedances and having identified them is the most important outcome of the bench measurements which we are reporting about. The other oscillations in the coupling impedance plot are due to the non perfect matching from the matching resistors and the fields bouncing back and forth between the two cavities. The negative impedance (unphysical for a passive device) corresponds to the $|S_{21}|$ greater than unity discussed above and it is due to reactive/inductive effects in the matching resistors.

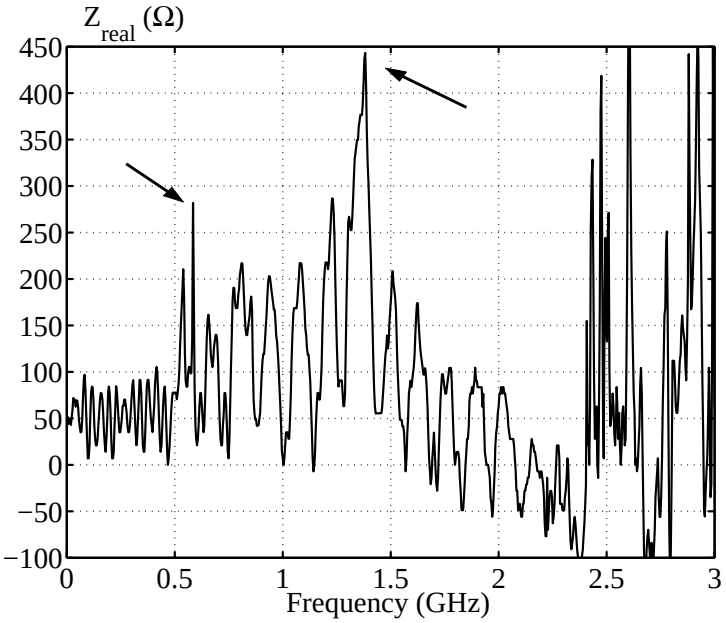

Figure 5: Real part of the longitudinal coupling impedance according to the "log formula". A copper wire (0.4 mm diameter) with matching resistors has been used. Interesting resonant modes are indicated by the arrows. The (unphysical) behaviour of the impedance at high frequency ($Z_{real} < 0$) is due to the frequency dependency of the resistor losses (no reference measurement available).

2.2 Rod measurements

In general, the thinner is the wire, the better the bench measurements reproduce the situation seen by the beam. The drawback of the thin wire is the increase in characteristic impedance of the transmission line and the resulting inaccuracy in measuring small impedances. Excluding the unexpected peaks, in fact, the impedance of the device is supposed to be small and thus a measurements with the rod was foreseen to give a better estimate of this value. Matching resistors were not used in this case in order to avoid unknown (frequency dependent) losses.

The second set of measurements (1 cm thick rod) lead to the same conclusions as for the thin wire set-up. Figure 6 shows the transmission coefficient S_{21} where again the two notches pointed by the arrows are due to the passive cavities mentioned above. As

there were no matching resistors used in this case, the magnitude of the S_{21} has not been corrected. On the contrary, the phase has been corrected according to the distance between the two DUT connectors, which amounts to about 1.08 m (this distance is smaller than before since there are no "SUCO box"[1)] units which would contain the matching resistors).

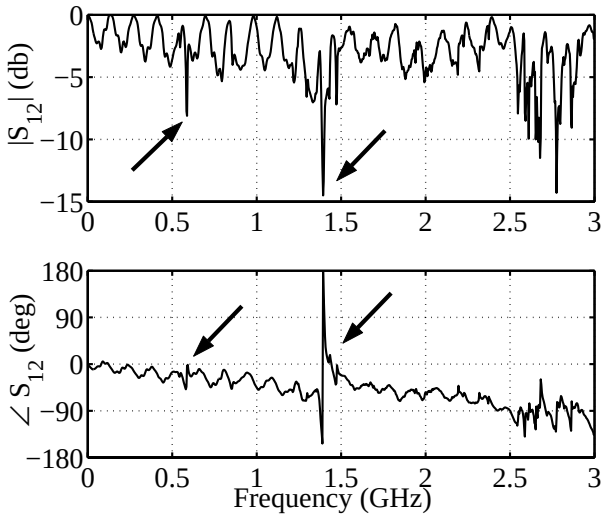

Figure 6: Transmission coefficient (S_{21}) versus frequency. A copper rod (10 mm diameter) is placed along the DUT axis. The upper plot shows the amplitude of the S_{21}, while the lower plot shows its phase, corrected according the distance between the two VNA connectors, that is 1.0777 m (time delay correction). The arrows indicate two (unexpected) resonances pointing to typical notches in the amplitude and jumps in the phase.

The characteristic impedance of the rod in the DUT is 132 Ω, according to numerical simulations of the actual set-up. This value was calculated by taking the minimum of the Z_{12} versus frequency; Z indicates the Z-matrix which can be derived directly from the HFSS simulations discussed below in sec. 2.3. Such a characteristic impedance is considerably different from the 50 Ω of the VNA ports and this mismatch is the reason of the undulations at low frequencies (say below 500 MHz) in Fig. 6.

The cavity related notches have the same frequencies as before. The absolute value may be slightly incorrect because of sampling inaccuracy. It is interesting to consider the phase jump of the second resonance: it amounts to (roughly) 360 degrees, indicating that the resonance is due to a 2 cavities coupled oscillation (a single cavity would have given a 180 degrees phase jump). The effect of the high order cavity modes and/or waveguide modes above 2.5 GHz is evident in Fig. 6 too.

Using the value of $Z_c = 132\ \Omega$ in the "log formula" of Eq. (1), the coupling impedance can be calculated and its real part Z_{real} is given in Fig. 7 in full agreement with Fig 5. The undulation is due to the mismatch between bench set-up and VNA and the minima are good indications for the coupling impedance at the frequencies where the minima are situated. The impedance is quite small as expected and it increases with frequency; anyway a precise quantitative estimation is questionable with the available data set-up.

[1)] Trade name of Huber+Suhner for a small housing with N connectors for individual components like a single resistor.

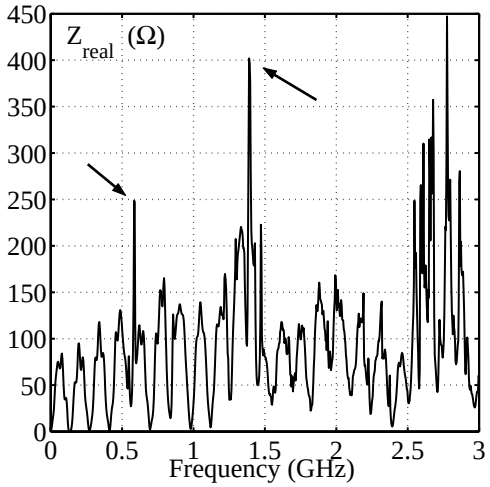

Figure 7: Real part of the longitudinal coupling impedance according to the "log formula". A copper rod (10 mm diameter) has been used. Interesting resonant modes are indicated by the arrows.

2.3 Parasite cavity: HFSS simulations

The main conclusion of the above measurement analysis is the presence of two undesired cavity-like resonances. To confirm that those peaks depends on the the contact region between the septum extremities and the tank flanges, the set-up (DUT + rod) has been studied numerically with HFSS. The aim of the simulations was to reproduce the S_{21} notches (or equivalently the impedance peaks) in order to check their origin.

The model used in the simulation is shown in Fig. 8. The septum itself is modelled by a "C-shaped" beam pipe: the cross section is an ellipse cut at 4/5 of its major semi-axis. The pieces of elliptical beam pipe on each side resemble the connection of the septum to the standard PS beam pipe (and their cross section is the non cut ellipse). The ellipse major axis is 163 mm and the minor one is 75 mm; the septum is assumed to be about 407 mm high (five times the major semi-axis) while the elliptical transitions are about 112 mm high (three times the minor semi-axis). The height of the septum is smaller than in reality, but this is irrelevant for the results we are interested in. More effort was required to make a realistic model of the contacts region (i.e. the cavities) which are the two flat parallelepipeds (295 mm×220 mm×17 mm) in Fig. 8. Each cavity is divided in two parts by the 3 mm thick metal sheet (grey region in Fig. 8) which has an opening of 253 mm×162 mm (the centre of this opening is 9 mm away in the x-direction with respect to the axis of the structure). Therefore, going from the elliptical pipes to the internal septum, one can recognise (inside the cavity region) first a free space of 7 mm, then the 3 mm thick metal sheet an then another 7 mm region. In this last region the metallic ridge (green part of Fig. 8) extends from the bottom of the metal sheet to the end of the cavity (i.e. it is 10 mm tall). The ridge and the metal sheet are not directly connected (see the 1 mm gap in Fig. 8.c) and this is believed to be important for the image current distribution. The copper rod (10 mm diameter) is placed in the centre of the structure and extends along the whole structure. The cavity external boundaries are declared as copper while the septum, the elliptical beam pipe walls, the metal sheet and the internal (green) ridge are perfect conductors.

The simulations have been carried out for a half structure (with magnetic wall

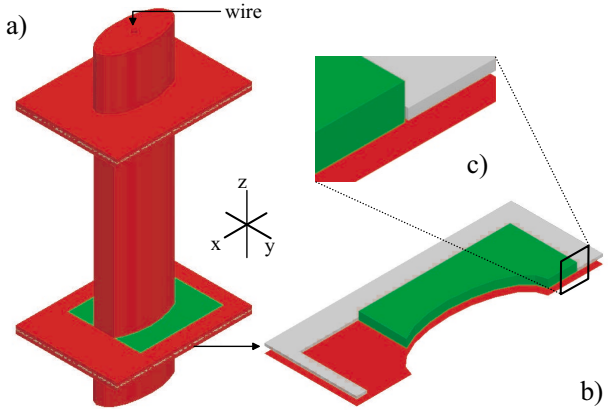

Figure 8: Model assumed in the HFSS simulation. The left picture a) shows the whole geometry: the septum itself is the "C" shaped pipe between the two passive cavities, resembling the contacts to the tank flanges. A metallic wire goes through all the structure. A detailed sketch of the lower contact region is in the right picture b) where the geometry has been cut along the xz-plane. The grey piece is a 3 mm thick metal sheet used to support the RF fingers located between the red plane (i.e. the lower side of the cavity) and the grey metal itself. The green part is also metallic and it mimics the shape of the actual support. There is a 1 mm gap between the metal sheet and the internal green metallic part, as shown in the picture c).

boundary condition on the xz-plane) using first manual meshing in the cavity region and then letting the program adaptively refine them. The magnitude (db) and phase of the transmission coefficient obtained is shown in Fig. 2.3. The low frequency notch (roughly at 780 MHz) is due to the metal sheet as well as the gap between the metal sheet and the ridge. The higher frequency resonances are present also without this metal sheet. The simulation agrees reasonably well with the network analyser data since it reproduces the notches seen in the measurements; the resonant frequencies, comparing VNA and HFSS results, agree reasonably well (e.g. for the lower frequency resonance we measure 580 MHz but the simulations give 780 MHz) and the 360 degrees phase jumps show up as well. Possible reasons of this non perfect agreement may be the fact that during the measurement the wire centre and the ellipse one are not the same (1 cm offset) as instead it is assumed in the simulations. Moreover in reality there are undefined contacts and the exact geometry of the transition has some details not included in the actual model (for practical reasons) which may induce a frequency shift.

3 Possible future improvements

The simulations reproduce to some extent the measured results and can be used to check ideas for possible improvements. The main goal is to find a way of removing the lower frequency peak in the coupling impedance which is well inside the relevant PS bunch spectrum.

A straightforward improvement include additional RF contacts at each end of the septum as close as possible to the beam axis, as shown in Fig. 10. Here the problem is to find a solution that is a compromise between theoretical desires (which would not allow any kind of radial gap) and what can be done practically including repair needs. It can never be excluded that the contacts get damaged during the mounting of the cover flange and then one must be able to change them quickly, possibly in a congested and

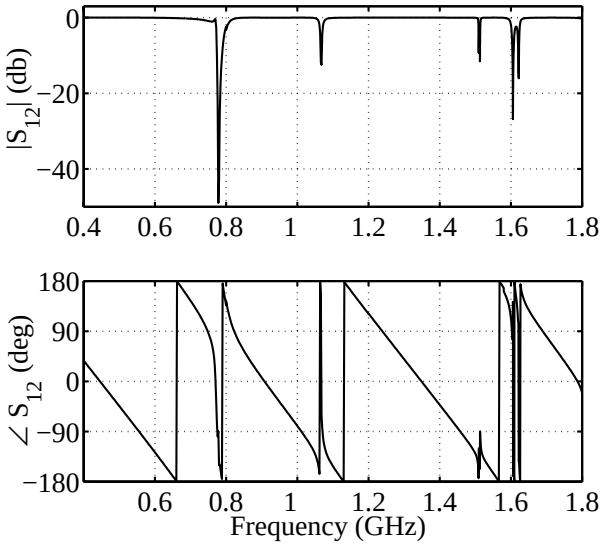

Figure 9: Transmission coefficient (S_{21}) versus frequency. The plots refer to a HFSS simulation of the bench measurement set-up (DUT with copper rod on its axis). The effect of the two passive cavities due the contacts between the septum extremities and the external flanges is clearly shown by the transmission notches. The 360 degrees phase jumps at some resonances show that the two cavities are coupled (by the TEM coaxial line). The frequencies of the notches do not match exactly the coupling impedance peaks, since for practical reasons it was not possible to simulate the exact geometry of the septum extremities.

radioactive environment. With all these constraints the solution shown in Fig. 10 appears still reasonable.

The proposed new contacts have been included in the HFSS model described earlier by simply inserting a 2D sheets (perfect conductor) connecting the metallic (green) ridge and the opposite cavity wall at the contact locations. The resulting S_{21} is shown in Fig. 11: there are no more significant resonances below 1.6 GHz.

4 Conclusion

The longitudinal beam coupling impedance of the septum PESEH23 has been evaluated using the coaxial wire method as well as HFSS simulations. As a result two major resonances were found in the frequency range up to 1.5 GHz. It turned out that close agreement between HFSS (wire) results and measurement was difficult to obtain since the cavities which give rise to these resonances have a very complicated shape and in addition undefined contacts. Nevertheless a reasonable agreement has been achieved. Further significant improvement appears possible by placing additional RF contact even closer to the beam despite considerable mechanical constraints. One of these constants is the requirement to be able to exchange such contacts with minimal effort in a radioactive environment if they are damaged. For the near and medium term future the impedance of septum 23 appears to be acceptable but the possibility of further upgrade should be used whenever this device is taken out of the ring.

5 Acknowledgements

The authors would like to thanks J. Borburgh, M. Hourican for all their help during the setup of the bench tests as well as providing many technical details and drawings

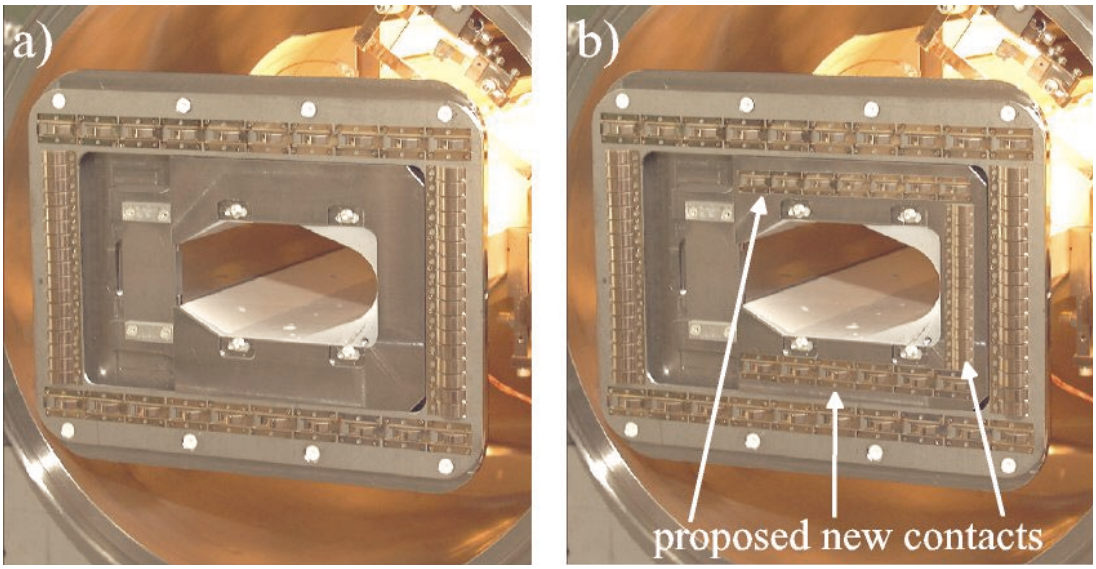

Figure 10: Septum extremity. The left photo represents the present situation where the electric contact between septum and the external flange is obtained with proper RF-contacts on the contour of the septum extremity. The right picture represents a proposal for positioning the new RF-contacts in order to reduce the coupling impedance seen by the beam. The optimum situation would be to have additional new contacts as close as possible to the beam pipe opening; the proposed solution is a compromise of this requirement with mounting issues of available contacts [5].

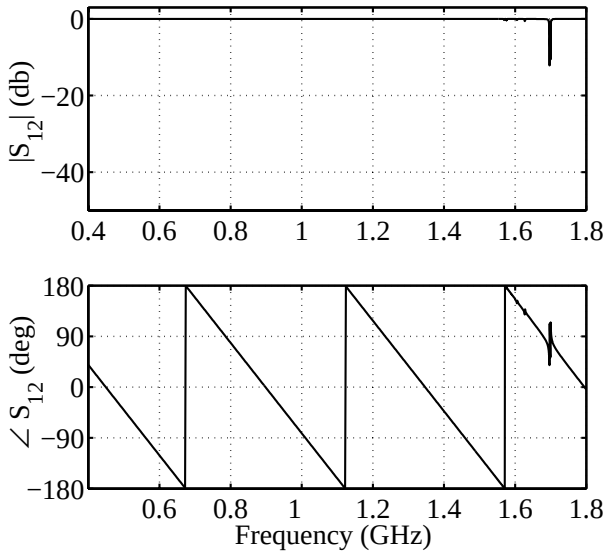

Figure 11: Transmission coefficient (S_{21}) versus frequency. The plots refer to HFSS simulations of the bench measurement set-up (DUT with copper rod on its axis), but including the newly proposed contacts. The most dangerous notch at low frequency disappeared and there are no more significant resonances below 1.6 GHz.

and their patience in discussions on possible further improvements. Thanks is also to R. Garoby and F. Pedersen for support and to E. Jensen and I. Syratchev for discussion.

References

[1] J. Borburgh, M. Hourican, M. Thivent, *Consolidation project of the electrostatic septa in the CERN PS ring*, IEEE Particle Accelerator Conference, Chicago, IL, USA, 18–22 Jun 2001, to be published; see also CERN-PS-2001-024-PO, June 2001.

[2] F. Caspers, *Impedance Determination from Bench Measurements*, Handbook of accelerator physics and engineering, A.W. Chao and M. Tigner (editors), World Scientific, Singapore, 1999.

[3] F. Caspers, A. Mostacci and B. Spataro, *On trapped modes in the LHC recombination chambers: experimental results*, LHC Project Note 266, CERN, August 2001.

[4] See World Wide Web address, `www.ansoft.com`.

[5] J. Borburgh, Private Communication (August 2001).